en
Experimental Neurobiology

Original Article

Temperature-induced Artifacts in Tau Phosphorylation: Implications for Reliable Alzheimer's Disease Research

Geoffrey Canet[1,2], Emma Rocaboy[1], Francis Laliberté[2], Emmanuelle Boscher[2], Isabelle Guisle[2],
Sofia Diego-Diaz[1], Parissa Fereydouni-Forouzandeh[1], Robert A. Whittington[3],
Sébastien S. Hébert[1,2], Vincent Pernet[1,4] and Emmanuel Planel[1,2*]

[1]*Department of Psychiatry and Neurosciences, Faculty of Medicine, Laval University, Québec G1V 4G2,*
[2]*Neurosciences Axis, Research Center of the CHU de Québec - Laval University, Québec G1V 4G2, Canada,*
[3]*Department of Anesthesiology and Perioperative Medicine, UCLA, Los Angeles, CA 90095, USA,*
[4]*Department of Neurology, Bern University Hospital, Bern 3010, Switzerland*

In preclinical research on Alzheimer's disease and related tauopathies, tau phosphorylation analysis is routinely employed in both cellular and animal models. However, recognizing the sensitivity of tau phosphorylation to various extrinsic factors, notably temperature, is vital for experimental accuracy. Hypothermia can trigger tau hyperphosphorylation, while hyperthermia leads to its dephosphorylation. Nevertheless, the rapidity of tau phosphorylation in response to unintentional temperature variations remains unknown. In cell cultures, the most significant temperature change occurs when the cells are removed from the incubator before harvesting, and in animal models, during anesthesia prior to euthanasia. In this study, we investigate the kinetics of tau phosphorylation in N2a and SH-SY5Y neuronal cell lines, as well as in mice exposed to anesthesia. We observed changes in tau phosphorylation within the few seconds upon transferring cell cultures from their 37°C incubator to room temperature conditions. However, cells placed directly on ice post-incubation exhibited negligible phosphorylation changes. In vivo, isoflurane anesthesia rapidly resulted in tau hyperphosphorylation within the few seconds needed to lose the pedal withdrawal reflex in mice. These findings emphasize the critical importance of preventing temperature variation in researches focused on tau. To ensure accurate results, we recommend avoiding anesthesia before euthanasia and promptly placing cells on ice after removal from the incubator. By controlling temperature fluctuations, the reliability and validity of tau phosphorylation studies can be significantly enhanced.

Key words: Tau phosphorylation, Neuronal cells, Temperature, C57BL6 mice, Anesthesia, Alzheimer's disease

INTRODUCTION

Alzheimer's disease (AD), the predominant form of neurodegenerative disease in the elderly, manifests through a progressive loss of cognitive function, leading to dementia [1]. AD is marked by two major neuropathological features: extracellular senile plaques composed of amyloid-beta (Aβ) peptide aggregates [2] and intracellular neurofibrillary tangles (NFTs) formed by aggregates of hyperphosphorylated microtubule-associated protein tau [1]. The biochemical assay of tau phosphorylation has thus become a mainstay to evaluate AD pathology, necessitating the development of various analytical methodologies in both basic and clinical research. However, the regulation of tau phosphorylation is a highly dynamic process influenced by numerous biological and environmental factors. Minimizing the impact of these factors is essential to avoid unintended phosphorylation artifacts and enhance the scientific rigor of experiments focusing on tau.

Variations in temperature, whether in animals or cell cultures,

pose a significant risk of introducing tau phosphorylation artifacts, and necessitates a careful calibration and monitoring. Tau phosphorylation is highly responsive to temperature changes, with hypothermia leading to tau hyperphosphorylation and hyperthermia causing tau dephosphorylation. Metabolic alterations in animal models, such as those induced by diabetes, starvation, or insulin treatment, can result in hypothermia-associated tau hyperphosphorylation [3-7]. Similarly, physiological variations in body temperature (BT) during sleep, torpor, or hibernation can also elevate phosphorylation levels [8-11]. Conversely, exposure to heat or thermogenesis-inducing drugs leads to tau dephosphorylation [12, 13]. In laboratory animals, anesthesia-induced hypothermia prior to euthanasia remains the most common source of temperature variation. Anesthesia has consistently been shown to directly and indirectly contribute to tau hyperphosphorylation [14-18]. In the case of cell cultures, the primary temperature fluctuation occurs when cells are removed from the incubator for extraction. However, the rapidity with which tau phosphorylation can change following these procedures is unknown.

This study aimed to examine the kinetics of tau hyperphosphorylation upon various periods of exposure to room temperature (RT) post-incubation. Proteins samples from two neuronal cell lines were collected at different time points (ranging from 30 seconds to 15 minutes) for tau analysis. The kinetic analysis of tau phosphorylation in mice following anesthesia was also conducted, as this procedure is commonly used prior euthanasia. As anesthesia is known to induce hypothermia [14, 19], mice were anesthetized with isoflurane and euthanized at various time points (from 0 to 15 minutes of anesthesia), while recording their rectal temperature.

The results revealed that tau phosphorylation was altered at specific epitopes within a few seconds following transfer to RT. Moreover, after just a few minutes of RT exposure, significant and widespread tau hyperphosphorylation occurred. Interestingly, hyperphosphorylation was prevented when cell cultures were immediately placed on ice, which inhibited kinase and phosphatase activities. Furthermore, we extended these findings to *in vivo* experiments, as anesthesia induced a pronounced and time-dependent hypothermia, which correlated with tau hyperphosphorylation at various sites in the mouse hippocampi and cortices. This study emphasizes the necessity of controlling temperature fluctuations in tau-related experiments to prevent artifactual data. To this end, we recommend the immediate placing of cells cultures on ice before sampling and the avoidance of anesthesia prior euthanasia in laboratory animals.

MATERIALS AND METHODS

Cell culture

In this study, two types of cells were used: SH-SY5Y cells stably expressing the human tau 3 repeat isoform 2+3-10 (referred to as SH3R cells, generously provided by Luc Buée, Inserm, Lille, France), and mouse Neuro2a cells (N2a) purchased from the American Type Culture Collection (ATCC #CRL-2266, Manassas, VA, USA). SH3R cells were cultured following previously established methods [20], while N2a cells were cultured according to the manufacturer's instructions. Both cell types were grown in DMEM/HIGH GLUCOSE medium (GE Healthcare Life Sciences, Logan, Utah, USA) supplemented with 10% bovine growth serum (Thermo Scientific, Logan, Utah, USA) and a mix of streptomycin/penicillin antibiotics. The cells were maintained in a 5% CO_2 humidified incubator at 37°C in either 6-well plates or 10 cm Petri dishes.

Animals

For the experiments, male and female C57BL6 mice, aged 8 weeks, were used (n=5 per group). The experimental procedures involving the mice were carried out in accordance with the guidelines provided by the Canadian Council on Animal Care and were approved by the "The Animal Care Committee of Université Laval" (CPAUL-3, approval number: CHU-22-1027)."

Experimental procedures

One group of mice served as the control (naive) group and did not undergo anesthesia. Other groups of mice were anesthetized with 3% isoflurane in oxygen (25%) inhaled in an induction chamber. Once the pedal reflex was lost (tail and paw pinch), the animals were euthanized immediately (t=0) or at specific time points of t=2 min, t=5 min, t=10 min, or t=15 min.

Temperature recordings

Before euthanasia, the core body temperature (BT) of mice was measured using a rectal probe (RET-3, Brain Tree Scientific Inc, Braintree, MA) connected to a digital thermometer (Thermalert TH5, Physitemp, Clifton, NJ). For recording the temperature of the cell medium, the same thermometer was utilized. The probe was immersed in the cell medium while keeping the 6-well plate closed.

Protein extraction and Western blotting

For experiments in SH3R and N2a cells, when full confluency was reached, the cells in 6-wells plates were removed from the incubator and were sampled immediately (t=0, control condition)

or at t=30 sec; 60 sec; 120 sec; 5 min; 10 min; 15 min (time spent at RT (21°C) or on ice). For cell extraction, the culture medium was removed, and the cells were washed twice with phospho-buffered saline 1x and collected in 100 µl of Radioimmunoprecipitation assay (RIPA) buffer and homogenized by sonication. For mouse experiments, the brains were promptly removed and tissues (hippocampi and cortices) were dissected on ice. Tissues were frozen using liquid nitrogen and stored at -80°C until homogenization. The hippocampi and cortices were homogenized by sonication in 150 or 200 µl of RIPA, respectively. Subsequently, all samples were centrifuged for 20 min at 20,000 g at 4°C. The supernatant was collected, diluted in sample buffer (NuPAGE LDS; Invitrogen, Carlsbad, CA) containing 5% of 2-β-mercapto-ethanol, 1 mM Na_3VO_4, 1 mM NaF, 1 mM PMSF, 10 µl/ml of Proteases Inhibitors Cocktail (P8340; Sigma-Aldrich, St. Louis, MO, USA), and heated for 10 min at 95°C. 10~20 µg of protein were then analyzed using previously described methods [21, 22]. The intensity of bands was quantified using ImageJ software (National Institutes of Health). β-actin was used as a loading control. Phospho-tau epitopes were normalized over Total tau. All the antibodies used for western blotting experiments and their dilutions are listed in Table 1. Representative lanes from the immunoblots were displayed for each specific experimental condition. The dashed lines indicate segments where certain lanes from the same blot were excluded, and the remaining lanes were combined. Brightness levels were adjusted as necessary to enhance visualization and accuracy.

Statistical analysis

For each condition, at least two distinct sets of experiments were performed. Before conducting any analysis of variance, the Gaussian distribution was evaluated and validated using the Kolmogorov-Smirnov test (GraphPad-Prism 5.0). The data are presented as mean±SEM and analyzed using one-way ANOVA followed by Dunnett's multiple comparison test (GraphPad-Prism 5.0). Statistical significance versus the control condition was denoted as follows: *=p<0.05, **=p<0.01, ***=p<0.01. Due to high variations in tau phosphorylation at later time points overshadowing subtle differences at early time points, a second one-way ANOVA was performed between the control condition and time points at 30 seconds, 60 seconds, and 120 seconds, followed by Dunnett's multiple comparison test. Statistical significance versus the control condition was denoted as follows: +=p<0.05, ++=p<0.01, +++=p<0.001. The results were then presented on the same graph.

Table 1. Antibodies used in Western blot experiments

Protein	Dilution	Supplier (catalog #)
Mouse primary antibodies		
AT270 (pThr181)	1/1,000	Thermo-Fisher (#MN1050)
CP13 (pSer202)	1/1,000	Peter Davies
AT100 (pThr212/pSer214)	1/1,000	Thermo-Fisher (#MN1060)
MC6 (pSer235)	1/1,000	Peter Davies
PHF1 (pSer396/pSer404)	1/1,000	Peter Davies
GSK3β	1/1,000	BD Biosciences (#610202)
Demethylated PP2AC	1/1,000	Santa Cruz (sc-13601)
PP2A, C subunit	1/1,000	Millipore (#05-545)
β-actin	1/10,000	Sigma-Aldrich (#A2228)
Rabbit primary antibodies		
pSer199	1/1,000	Thermo-Fisher (#44734G)
pThr205	1/1,000	Thermo-Fisher (#44738G)
pSer262	1/1,000	Thermo-Fisher (#44750G)
pSer409	1/1,000	Thermo-Fisher (#44760G)
pSer422	1/1,000	Thermo-Fisher (#44774G)
Total tau (TauC)	1/10,000	Dako Cytomation (#A0024)
pGSK3β (Ser9)	1/1,000	Cell Signaling (#9336)
HSP70	1/1,000	Cell Signaling (#4872S)
HSP90	1/1,000	Cell Signaling (#4877S)
SAPK/JNK	1/1,000	Cell Signaling (#9252S)
pThr183/Tyr185 SAPK/JNK	1/1,000	Cell Signaling (#9251S)
Secondary antibodies		
Goat anti-mouse IgG HRP conjugate (HC+LC)	1/5,000	Jackson laboratories (#115-035-003)
Goat anti-mouse IgG HRP conjugate (LC specific Ab)	1/5,000	Millipore (#AP200P)
Goat anti-rabbit IgG HRP conjugate (HC+LC)	1/5,000	Jackson laboratories (#111-035-144)

RESULTS

Rapid changes in tau phosphorylation level in SH3R cells exposed to room temperature

The primary objective of this study was to investigate the kinetics of tau phosphorylation in SH3R neuronal cells when exposed to RT (*21℃*) subsequent to their removal from their 37°C incubator (Fig. 1a). Tau phosphorylation level was assessed using specific antibodies targeting phosphorylated tau at distinct epitopes, including AT270 (pThr181) [23], pSer199, CP13 (pSer202) [24], pThr205, AT100 (pThr212/pSer214) [25], MC6 (pSer235) [26], pSer262, PHF1 (pSer396/pSer404) [27], pSer409, and pSer422 (Table 1). These particular tau antibodies were chosen due to their relevance to AD-related pathological processes, such as pretangle formation (CP13), paired helical filament and NFT formation (pSer202/pThr205, PHF1) [23, 28], as well as the disruption of tau binding to microtubules (pSer262) [29]. All other phosphoepitopes were found to exhibit abnormal phosphorylation patterns in the AD brain [30]. Therefore, these antibodies were deemed appropriate for providing a comprehensive assessment of the impact of RT exposure on tau phosphorylation. Notably, we observed a significant decline in the cell medium temperature immediately post-exposure to RT, with a decrease of -0.78°C within 30 seconds, progressively declining to an average of 25.33°C after 15 minutes (Fig. 1b). Considering the substantial variability in tau phosphorylation at later time points, which masked more nuanced early changes, we conducted a second one-way ANOVA between the control condition and time points at 0.5, 1 and 2 min. Remarkably, three epitopes, pSer199 (*+37.3%*), MC6 (*+60.8%*) and pSer262 (*+49.1%*), showed acute hyperphosphorylation, detectable as early as 30 seconds (Fig. 1d, h, i). Moreover, tau exhibited hyperphosphorylation at AT100 (*+31.6%*) and pSer422 (*+32.3%*) after 60 seconds (Fig. 1g, l).

The majority of tau epitopes examined exhibited hyperphosphorylation whithin 5 minutes post-transition to RT, including AT270 (*+69.9%*), AT100 (*+50.5%*), pSer262 (*+78%*), and pSer422 (*+103.4%*) (Fig. 1c, g, i, l), with sustained phosphorylation up to 10 or 15 minutes, except for pSer199 (Fig. 1d). Additionally, following the 15-minute time frame, the activities of JNK (*+199.5%*) and GSK3β (*-51.99%*) significantly increased, alongside an inactivation of PP2A (*+106.5%*) (Fig. 2a~c). Surprisingly, CP13, pThr205, and PHF1 epitopes displayed biphasic changes, with dephosphorylation in the first few time points followed by subsequent hyperphosphorylation at 15 min (Fig. 1e, f, j). Collectively, these observations underscore the rapid modulation of tau phosphorylation at multiple epitopes upon RT exposure in SH3R cells.

We examined the correlations between phosphorylation intensities at each epitope and the time elapsed post-incubation (Fig. 3a, b). Several epitopes, including pSer422, AT100, AT270, pSer409, pThr205, and CP13, correlated positively with sampling time, while total tau levels remained unchanged. Additionally, an inverse relationship was evidenced between tau hyperphosphorylation and the decline in cell medium temperature, as illustrated for epitopes pSer422, AT100, AT270, pSer409, and pThr205 (Fig. 3c, d).

Rapid changes in kinases and phosphatases in SH3R cells exposed to room temperature

To explore the underlying mechanism of tau phosphorylation changes, we assessed the expression levels of HSP70 and HSP90 (Heat Shock Proteins), chaperones known for their response to thermal stress, and their role in tau phosphorylation, aggregation and degradation [31]. However, we did not observe any significant alterations in the expression of these two chaperones over time (from t=0 to t=15 minutes) following exposure to RT (Fig. 2d, e), suggesting a limited role in tau phosphorylation regulation under our experimental conditions. We also investigated the activities of GSK3β (Glycogen Synthase Kinase 3β) and JNK (c-Jun N-terminal kinase), both of which are recognized as major tau kinases, as well as PP2A (Protein Phosphatase 2A), the principal tau phosphatase [32, 33]. JNK is activated in response to various stress stimuli through phosphorylation at Thr183 and Tyr185 [34]. Conversely, GSK3β primary regulation occurs through inhibitory phosphorylation at the Ser9 residue [35]. PP2A is responsible for approximately 70% of tau dephosphorylation and is activated by the methylation of its catalytic subunit [32]. Most tau phosphoepitopes investigated here are substrate of both kinases and PP2A [32, 33]. We observed that the rapid hyperphosphorylation of some tau epitopes coincided with the swift activation of JNK (within 30 seconds, *+62.4%*) and GSK3β (dephosphorylation at Ser9 after 60 seconds, *-20.84%*), as well as the inactivation of PP2A (demethylation after 60 seconds, *+31.98%*) (Fig. 2a~c). Furthermore, over the 15-minute timeframe, the activation of JNK (*+199.5%*) and GSK3β (*-51.99%*) increased significantly, while PP2A demethylation was augmented (*+106.5%*) (Fig. 2a~c). These results suggest that temperature may directly influence enzyme kinetics and also trigger kinase activation and PP2A inhibition pathways rapidly post-RT exposure. However, our findings fail to explain the dephosphorylation of tau occurring within the first minutes for epitopes such as CP13, pThr205 and PHF1.

Increase in tau phosphorylation in N2a cells exposed to room temperature

To validate our findings in another neuronal cell line expressing endogenous tau, we used mouse neuroblastoma N2a cells
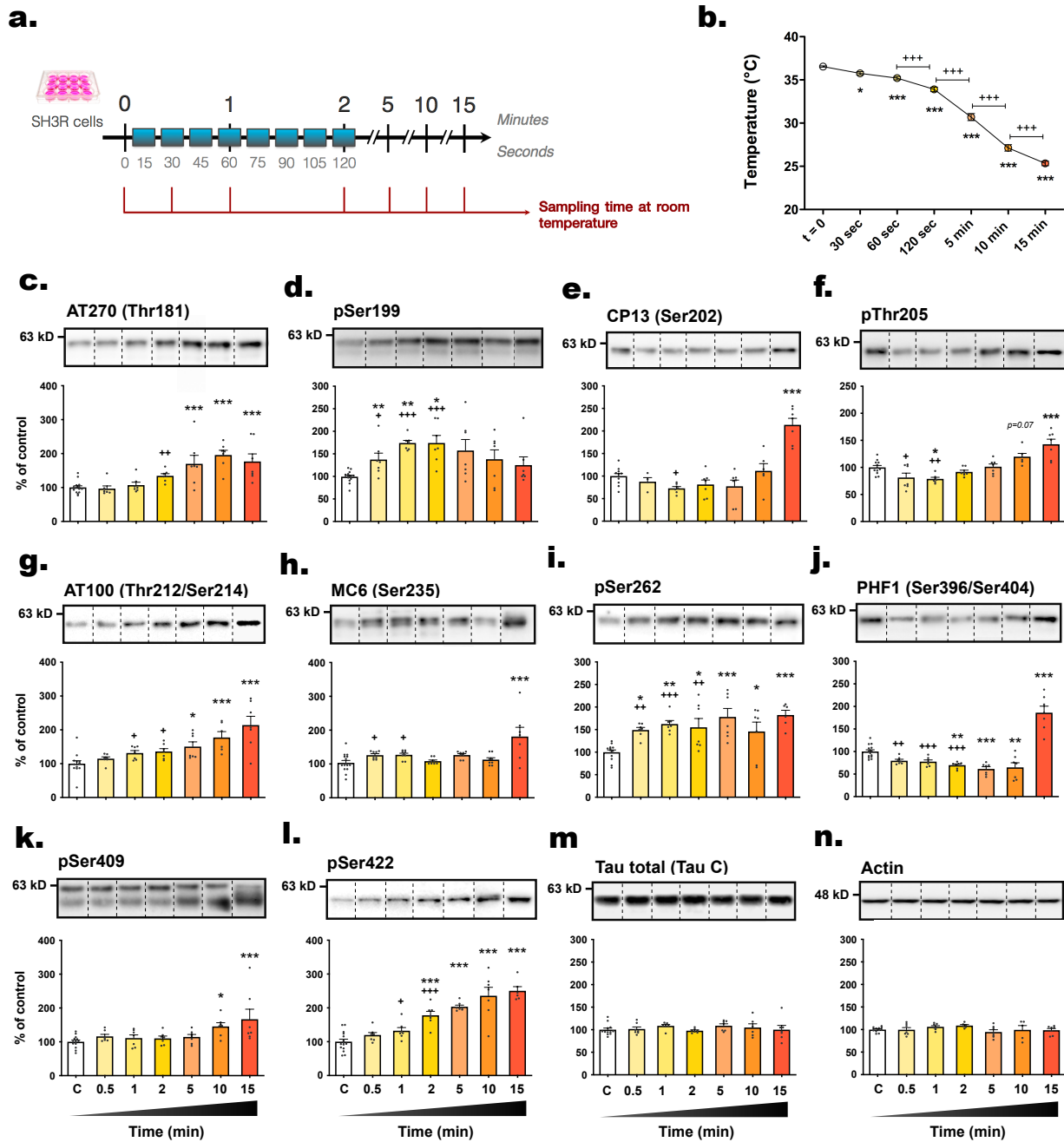
Fig. 1. The level of tau phosphorylation in SH3R cells is rapidly influenced by exposure to room temperature. (A) Experimental protocol. Cells in 6-wells plates were removed from incubators and were sampled immediately (t=0, control) or at 0.5; 1; 2; 5; 10; 15 min (time spent at RT). (B) Measurement of the temperature of cell medium (when removed from the incubator) against time. Repeated measures 1-way ANOVA followed by Tukey's post-test was performed, $F_{6,30}=18.20$ (p<0.05). *p<0.05, **p<0.01 and ***p<0.001 vs. control condition; +++p<0.001 vs. indicated group. n=6 per condition. The following antibodies were probed by immunoblot: (C) AT270 (pThr181), (D) pSer199, (E) CP13 (pSer202), (F) pThr205, (G) AT100 (pThr212/Ser214), (H) MC6 (pSer235), (I) pSer262, (J) PHF1 (pSer396/404), (K) pSer409, (L) pSer422, (M) total tau and (N) β-actin. For immunoblot quantification, each phospho-epitope level was normalized over total tau protein levels. For each condition, a representative band is presented above graphs. Data are presented as mean±SEM and expressed as percentage of control condition (t=0). n=6~10 per condition. 1-way ANOVAs followed by Dunnett's post-test were performed: AT270: $F_{6,50}=9.96$ (p<0.001); pS199: $F_{6,50}=4.54$ (p<0.001); CP13: $F_{6,42}=20.89$ (p<0.0001); pT205: $F_{6,46}=14.32$ (p<0.0001); AT100: $F_{6,47}=8.87$ (p<0.0001); MC6: $F_{6,55}=6.34$ (p<0.0001); pS262: $F_{6,47}=5.92$ (p<0.0001); PHF1: $F_{6,49}=36.35$ (p<0.0001); pS409: $F_{6,48}=3.89$ (p<0.01); pS422: $F_{6,49}=25.96$ (p<0.0001); total tau: $F_{6,46}=0.67$ (ns); actin: $F_{6,44}=1.29$ (ns). *p<0.05, **p<0.01 and ***p<0.001 vs. control condition. A second 1-way ANOVA followed by Dunnett's post-test was performed only on the first timings (from t=0 to t=120 sec) : AT270: $F_{3,32}=6.05$ (p<0.01); pS199: $F_{3,32}=17.78$ (p<0.0001); CP13: $F_{3,26}=3.19$ (p<0.05); pT205: $F_{3,29}=4.74$ (p<0.01); AT100: $F_{3,30}=4.21$ (p<0.05); MC6: $F_{3,35}=4.07$ (p<0.05); pS262: $F_{3,30}=10.84$ (p<0.0001); PHF1: $F_{3,31}=13.85$ (p<0.001); pS409: $F_{3,26}=0.97$ (ns); pS422: $F_{3,32}=13.63$ (p<0.0001). +p<0.05, ++p<0.01 and +++p<0.001 vs. control condition.
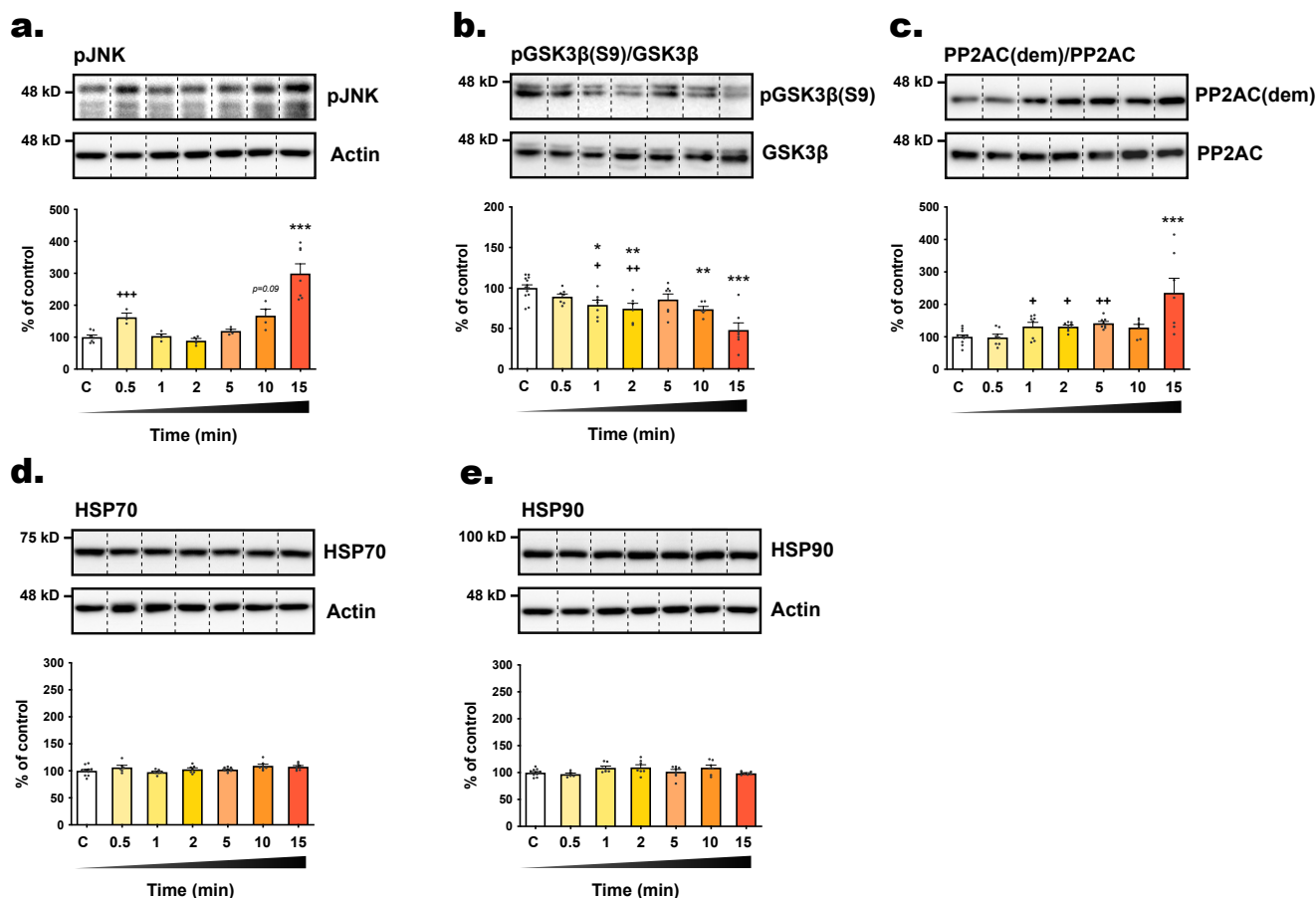
Fig. 2. Influence of room temperature exposure on tau-related enzymes and chaperones. The expression level of (A) ratio of inactive pGSK3β(pSer9)/GSK3β, (B) ratio of pJNK/JNK, (C) ratio of inactive demethylated PP2AC/PP2AC, (D) HSP70 and (E) HSP90 were determined by Western blot in cells harvested immediately (t=0, control) or at t=0.5; 1; 2; 5; 10; 15 min (time spent at RT). HSP70 and HSP90 were normalized over actin levels. For each condition, a representative band is presented above graphs. Data are presented as mean±SEM and expressed as percentage of control condition (t=0). 1-way ANOVAs followed by Dunnett's post-test were performed: RT pGSK3β(pSer9): $F_{6,46}$=9.22 (p<0.0001); pJNK: $F_{6,26}$=18.02 (p<0.05); demethylated PP2AC: $F_{6,51}$=5.712 (p<0.0001); HSP70: $F_{6,45}$=2.48 (p<0.0001); HSP90: $F_{6,45}$=2.47 (p<0.05); ice pGSK3β(pSer9): $F_{6,45}$=1.23 (ns). *p<0.05, **p<0.01 and ***p<0.001 vs. control condition. A second 1-way ANOVA followed by Dunnett's post-test was performed only on the first timings (from t=0 to t=5 min): pGSK3β(pSer9): $F_{4,35}$=4.13 (p<0.01); pJNK: $F_{4,17}$=10.59 (p<0.001); demethylated PP2AC: $F_{4,39}$=6.58 (p<0.001); HSP70: $F_{4,33}$=1.37 (ns); HSP90: $F_{4,33}$=2.57 (ns). +p<0.05, ++p<0.01 and +++p<0.001 vs. control condition.

and followed the same protocol (Fig. 4a). Within 30 seconds of RT exposure, tau hyperphosphorylation was observed at AT270 (+*52.1%*) and pSer409 epitopes (+*62.6%*) (Fig. 4b, f). All epitopes displayed hyperphosphorylation after 5 minutes, including AT270 (+*89.9%*), pSer199 (+*30.1%*), CP13 (+*75.2%*), pThr205 (+*64.2%*), and pSer409 (+*74.7%*) (Fig. 4b~f), and persisting up to 15 minutes. While CP13 and pThr205 showed progressive increases in phosphorylation (Fig. 4d, e), the subsequent decrease observed in SH3R cells (Fig. 1d, e) was absent, suggesting cell-line specific regulatory mechanisms or thermal adaptivity. Interestingly, the second one-way ANOVA performed between the first three time points revealed swift hyperphosphorylation of tau at pThr205 and pSer409 after 60 seconds (Fig. 4e, f) and at pSer199 after 120 seconds (Fig.

4c).

Placing cell plates on ice prevents tau hyperphosphorylation

Ice is commonly used to prevent protein and RNA degradation in laboratory experiments by inhibiting enzymatic activities. Therefore, we immediately placed SH3R cell plates on ice post-transition to RT to evaluate its efficacy in preventing tau hyperphosphorylation (Fig. 5a). This approach successfully prevented tau hyperphosphorylation at several epitopes, including pSer199, CP13, AT100, and pSer409 (Fig. 5c, d, f, j), and blocked GSK3β activation (Fig. 5n), although variability increased with longer post-incubation time spans. Surprisingly, we observed a significant
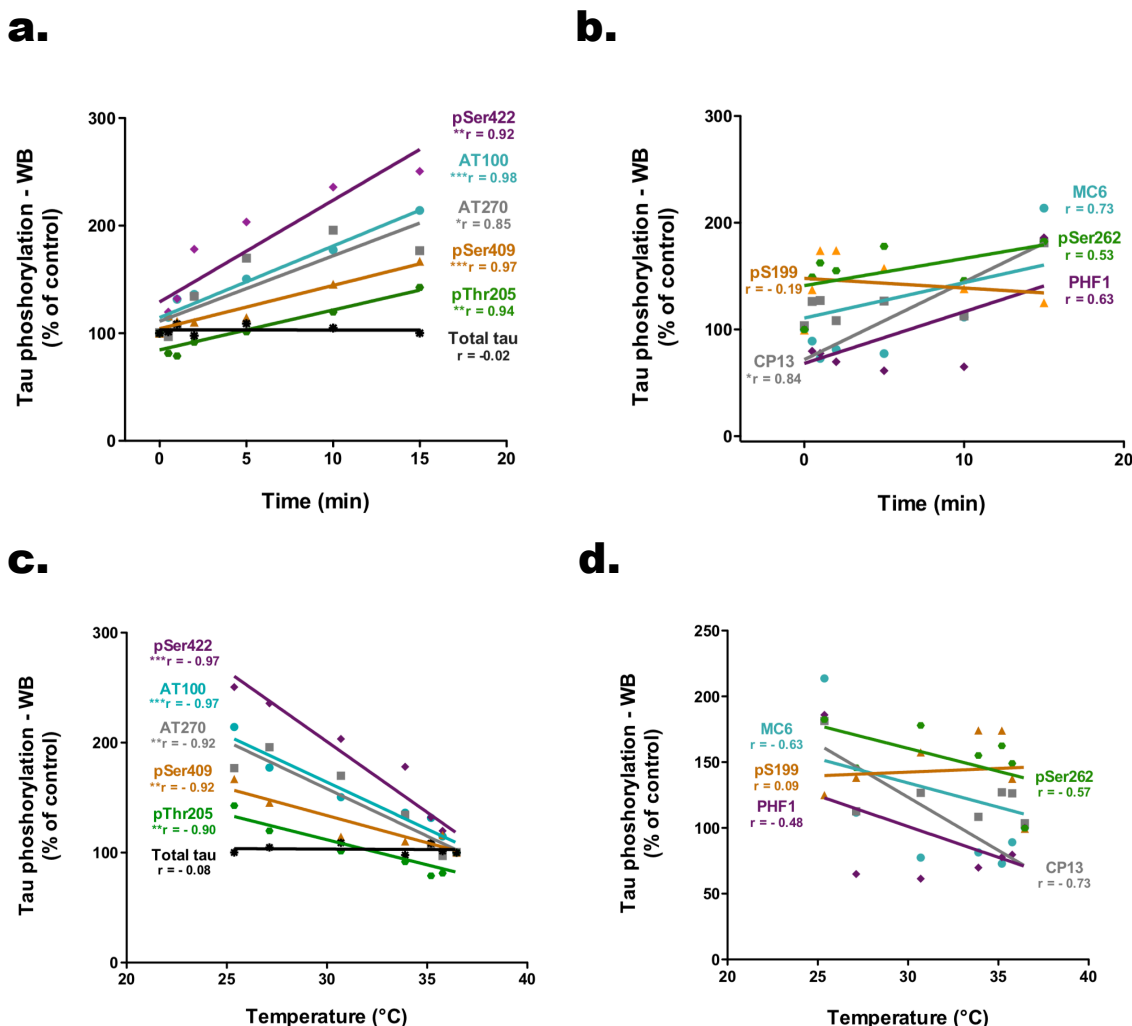
Fig. 3. Significant correlation between tau hyperphosphorylation in SH3R cells and the duration of post-incubation sampling as well as the temperature of the cell medium. (A, B) Correlation between Tau phosphorylation level modification and time (for the following epitopes: pSer422, AT100, AT270, pSer409, pThr205, pSer199, CP13, MC6, pSer262, PHF1 and total tau). Each point represents the mean of the values obtained with immunoblot quantification. Statistical relationships were calculated with the *r* Pearson's correlation coefficient (*r* values are indicated below each marker). *p<0.05, **p<0.01 and ***p<0.001. (C, D) Correlation between tau phosphorylation level modification and the mean temperature of cell medium (for the following epitopes: pSer422, AT100, AT270, pSer409, pThr205, pSer199, CP13, MC6, pSer262, PHF1 and total tau). Each point represents the mean of the values obtained with immunoblot quantification. Statistical relationships were calculated with the *r* Pearson's correlation coefficient (*r* values are indicated below each marker). *p<0.05, **p<0.01 and ***p<0.001.

decrease in PHF1 signal at 5 (*-29.36%*) and 10 (*-18.91%*) minutes.

However, while the variations were lower than those observed in Fig.1, tau phosphorylation remained significantly increased at some epitopes at later time points: pThr205 (*+39.5%*) and pSer422 (*+42.6%*) after 10 minutes (Fig. 5e, k); and pSer262 (*+53.9%*) after 15 minutes (Fig. 5h). The rapid increase in MC6 phosphorylation (*+26.1% at 30 seconds and +24.7% at 60 seconds*) (Fig. 5g) was not prevented by ice, suggesting a more complex regulatory mechanism. In conclusion, placing cell plates on ice before protein extraction limited tau hyperphosphorylation, although some epi-

topes still exhibited increased phosphorylation after some post-incubation time spans.

Anesthesia-induced hypothermia increases tau phosphorylation

We further investigated the impact of anesthesia-induced hypothermia on tau phosphorylation kinetics. Anesthesia induced by inhalation of 3% isoflurane (vaporized in an induction chamber) caused a rapid and time-dependent decrease in the BT of mice (Fig. 6b). The time point for mice to be deeply anesthetized (t=0) was
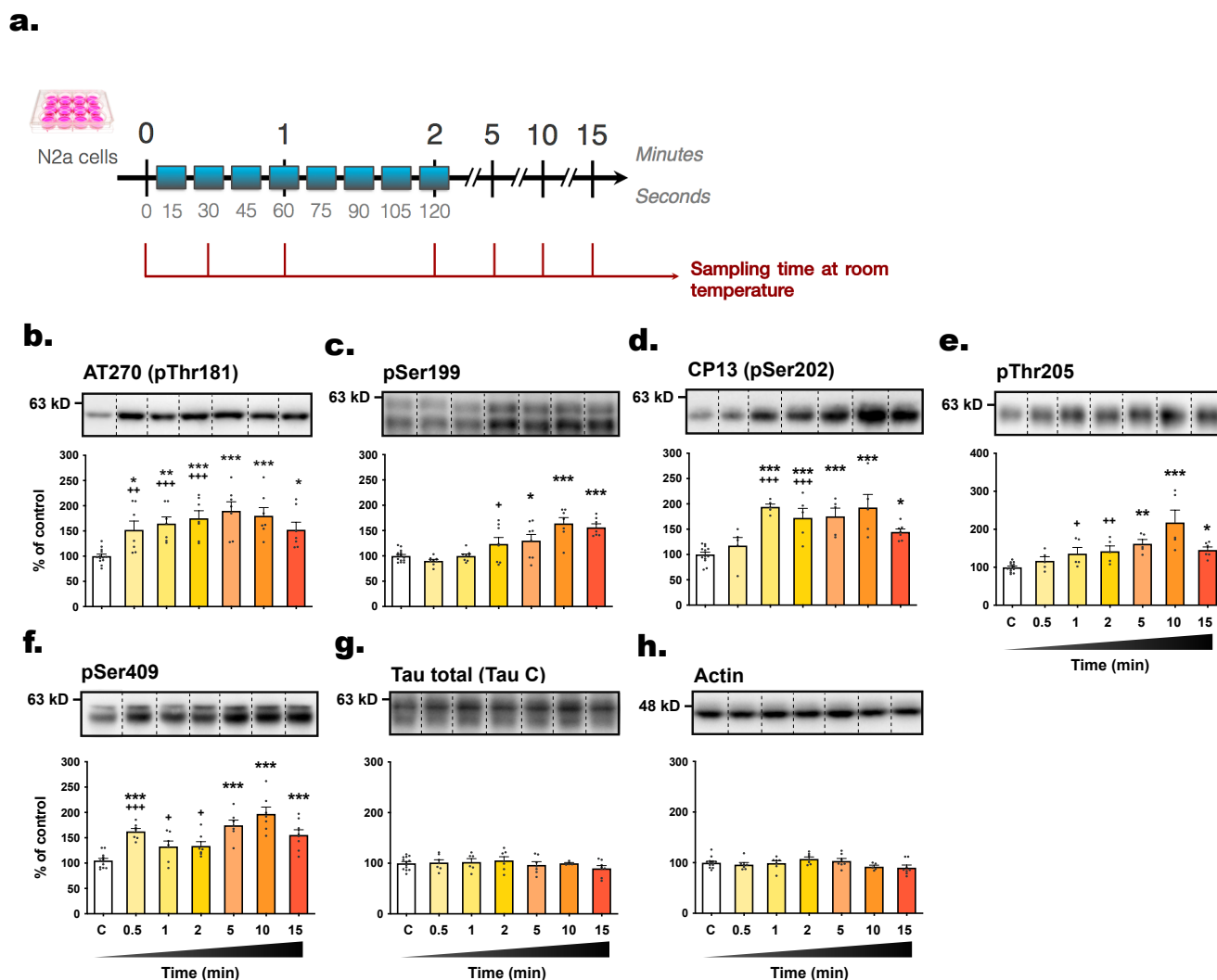
Fig. 4. The level of tau phosphorylation in N2a cells is rapidly affected by exposure to room temperature. (A) Experimental protocol. Cells in 6-wells plates were removed from incubators and were sampled immediately (t=0, control condition) or at t=0.5; 1; 2; 5; 10; 15 min (time spent at RT). The following antibodies were probed by immunoblot: (B) AT270 (pThr181), (C) pSer199, (D) CP13 (pSer202), (E) pThr205, (F) pSer409, (G) total tau and (H) β-actin. For each condition, a representative band is presented above graphs. For immunoblot quantification, each phospho-epitope level was normalized over total tau protein levels. Data are presented as mean±SEM and expressed as percentage of control condition (t=0). 1-way ANOVAs followed by Dunnett's post-test were performed: AT270: $F_{6,48}$=6.70 (p<0.0001); pS199: $F_{6,54}$=12.92 (p<0.0001); CP13: $F_{6,38}$=10.85 (p<0.0001); pT205: $F_{6,38}$=9.38 (p<0.0001); pS409: $F_{6,48}$=13.21 (p<0.0001); total tau: $F_{6,46}$=0.83 (ns); actin: $F_{4,47}$=1.91 (ns). *p<0.05, **p<0.01 and ***p<0.001 vs control condition. n=6~10 per condition. A second 1-way ANOVA followed by Dunnett's post-test was performed only on the first timings (from t=0 to t=120 sec) : AT270: $F_{3,31}$=11.69 (p<0.0001); pS199: $F_{3,35}$=4.84 (p<0.01); CP13: $F_{3,30}$=11.70 (p<0.0001); pT205: $F_{3,31}$=4.85 (p<0.01); pS409: $F_{3,29}$=12.56 (p<0.0001). +p<0.05, ++p<0.01 and +++p<0.001 vs. control condition.

determined by the loss of pedal reflex (tail and paw pinch). This phenomenon occurred within a minute of isoflurane exposure, and coincided with a significant BT drop (*-1.2℃*), progressively diminishing as much as 7.8℃ within 15 minutes (Fig. 6b).

We then separately examined the hippocampus and cortex, the two main structures involved in Alzheimer's disease (AD) [36]. Similar changes in tau hyperphosphorylation were observed in both hippocampus and cortex tissues. With the exception of

pSer409 (Fig. 6h), all epitopes assessed, including AT270, pSer199, CP13, pThr205, and PHF1, showed hyperphosphorylation after 10 or 15 minutes of anesthesia. Notably, tau hyperphosphorylation occurred more promptly in the hippocampus at AT270 (*2 minutes in the hippocampus, 10 minutes in the cortex*) (Fig. 6c), CP13 (*t=0 in the hippocampus, 10 minutes in the cortex*) (Fig. 6e), and PHF1 epitopes (*2 minutes in the hippocampus, 10 minutes in the cortex*) (Fig. 6g), suggesting greater sensitivity to hypothermic conditions
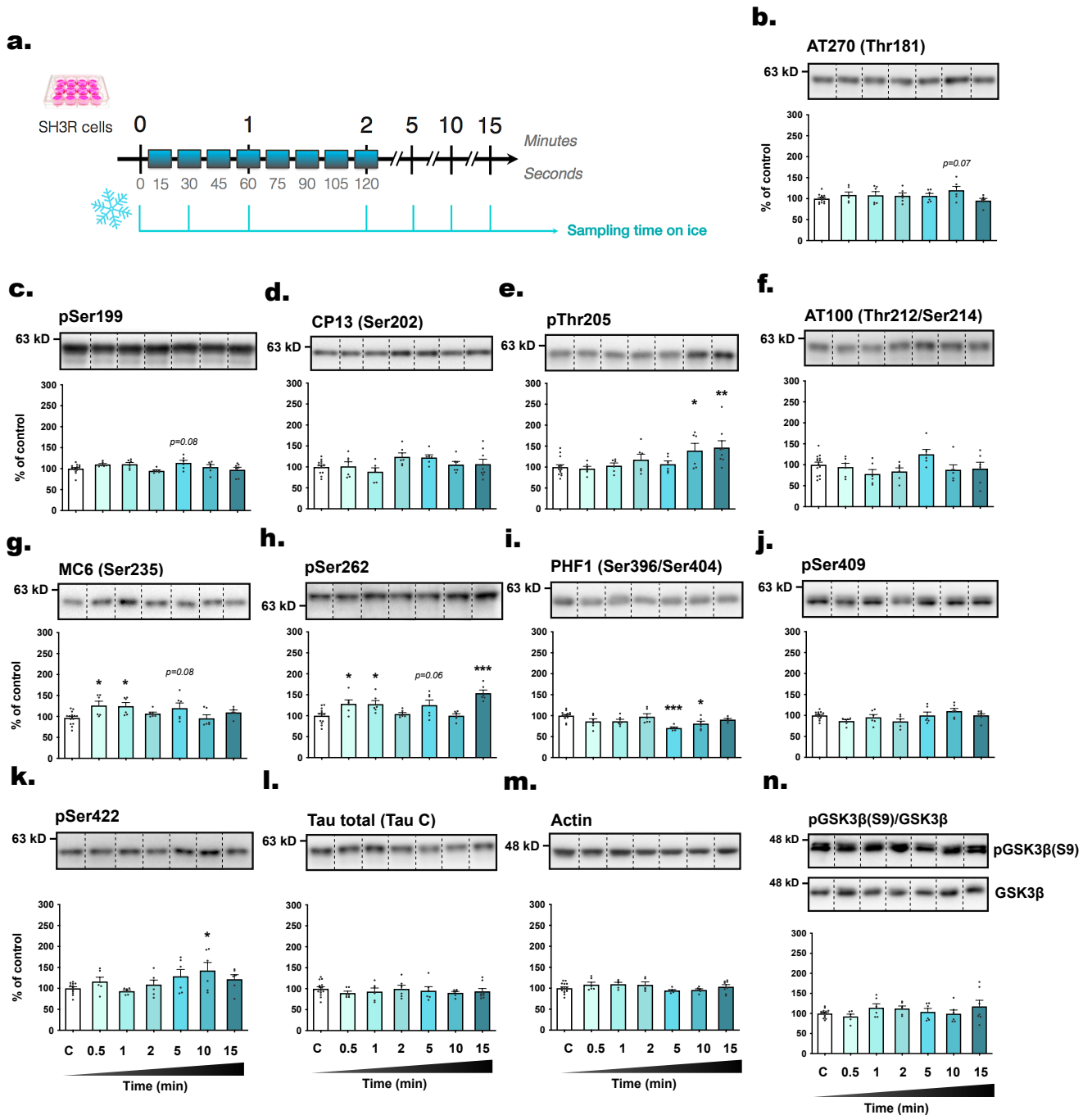
Fig. 5. Putting SH3R cell plates on ice blocked the induction of tau phosphorylation following removal from the incubator. (A) Experimental protocol. Cells in 6-wells plates were removed from incubators and were sampled immediately (t=0, control) or at t=0.5; 1; 2; 5; 10; 15 min (time spent on ice). The following antibodies were probed by immunoblot: (B) AT270 (pThr181), (C) pSer199, (D) CP13 (pSer202), (E) pThr205, (F) AT100 (pThr212/Ser214), (G) MC6 (pSer235), (H) pSer262, (I) PHF1 (pSer396/404), (J) pSer409, (K) pSer422, (L) total tau and (M) β-actin and (N) ratio of inactive pGSK3β(pSer9)/GSK3β. For each condition, a representative band is presented above graphs. For immunoblot quantification, each phospho-epitope level was normalized over total tau protein levels. Data are presented as mean±SEM and expressed as percentage of control condition (t=0). 1-way ANO-VAs followed by Dunnett's post-test were performed: AT270: $F_{6,42}=1.61$ (ns); pS199: $F_{6,45}=2.67$ (p<0.05); CP13: $F_{6,46}=2.07$ (ns); pT205: $F_{6,45}=3.53$ (p<0.01); AT100: $F_{6,43}=2.00$ (ns); MC6: $F_{6,43}=3.27$ (p<0.01); pS262: $F_{6,42}=7.26$ (p<0.0001); PHF1: $F_{6,42}=5.34$ (p<0.001); pS409: $F_{6,45}=2.67$ (p<0.05); pS422: $F_{6,41}=2.52$ (p<0.05); total tau: $F_{6,45}=0.42$ (ns); actin: $F_{6,44}=1.66$ (ns); pGSK3β(pSer9): $F_{4,34}=2.05$ (ns). *p<0.05, **p<0.01 and ***p<0.001 vs. control condition. n=6~10 per condition.
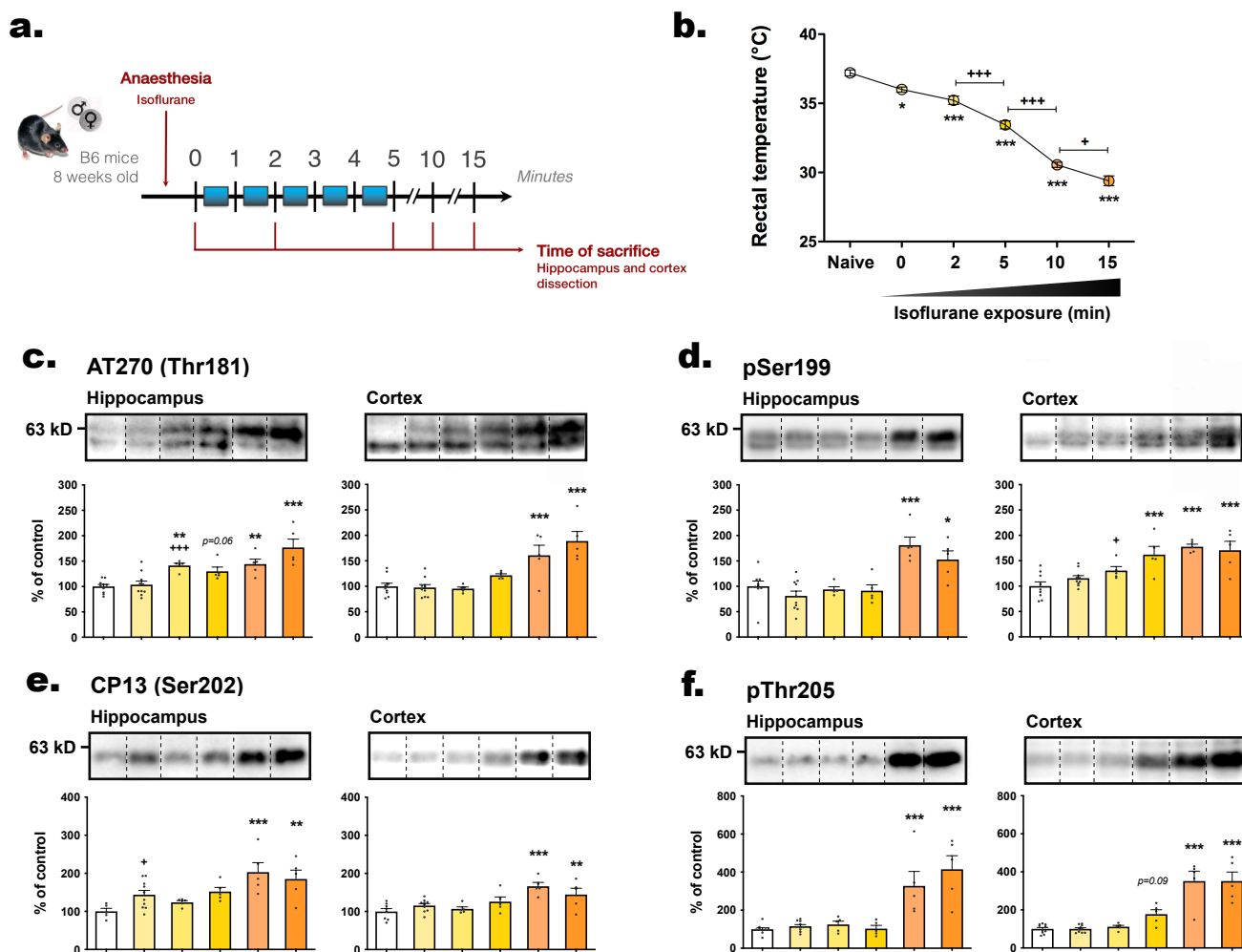
Fig. 6. Tau hyperphosphorylation occurs after hypothermia induced by anesthesia. (A) Experimental protocol. C57BL6 mice (both males and females) were euthanatized by decapitation immediately (naive, control condition) or after exposure to isoflurane: t=0 (deep sleep); 2; 5; 10; 15 min. Brains were immediately removed and hippocampi and cortices were dissected and frozen for Western blot analysis. (B) Just before euthanasia, rectal temperature was assessed. 1-way ANOVA followed by Tukey's post-test was performed, $F_{5,24}=139.6$ (p<0.0001). *p<0.05 and ***p<0.001 vs. naive. +p<0.05 and +++p<0.001 vs. indicated group. n=5 per group. The following antibodies were probed by immunoblot: (C) AT270 (pThr181), (D) pSer199, (E) CP13 (pSer202), (F) pThr205, (G) PHF1 (pSer396/404), (H) pSer409, (I) total tau and (J) β-actin. For each condition, a representative band is presented above graphs. For immunoblots quantification, each phospho-epitope level was normalized over total tau protein levels. Data are presented as mean±SEM and expressed as percentage of control condition (naive). n=5~10 per condition. For each hippocampus and cortex analysis, a 1-way ANOVA followed by Dunnett's post-test was performed: Hippocampus AT270: $F_{5,34}=12.41$ (p<0.0001); Cortex AT270: $F_{5,34}=13.73$ (p<0.0001); Hippocampus pS199: $F_{5,33}=10.26$ (p<0.0001); Cortex pS199: $F_{5,33}=10.80$ (p<0.0001); Hippocampus CP13: $F_{5,29}=5.33$ (p<0.01); Cortex CP13: $F_{5,32}=6.81$ (p<0.001); Hippocampus pT205: $F_{5,34}=14.92$ (p<0.0001); Cortex pT205: $F_{5,34}=25.23$ (p<0.0001); Hippocampus PHF1: $F_{5,29}=20.90$ (p<0.0001); Cortex PHF1: $F_{5,33}=20.90$ (p<0.0001); Hippocampus pS409: $F_{5,34}=5.42$ (p<0.001); Cortex pS409: $F_{5,34}=9.88$ (p<0.0001); Hippocampus total tau: $F_{5,24}=0.74$ (ns); Cortex total tau: $F_{5,24}=0.71$ (ns); Hippocampus actin: $F_{5,24}=0.75$ (ns); Cortex actin: $F_{5,24}=2.23$ (ns) vs. naive. *p<0.05, **p<0.01 and ***p<0.001 vs. control condition. A second 1-way ANOVA followed by Dunnett's post-test was performed only on the first groups (naive, t=0 and t=2 min): Hippocampus AT270: $F_{2,22}=10.84$ (p<0.0001); Cortex AT270: $F_{2,22}=0.12$ (ns); Hippocampus pS199: $F_{2,21}=1.10$ (ns); Cortex pS199: $F_{2,21}=3.80$ (p<0.05); Hippocampus CP13: $F_{2,17}=4.01$ (p<0.05); Cortex CP13: $F_{2,20}=1.84$ (ns); Hippocampus pT205: $F_{2,22}=1.52$ (ns); Cortex pT205: $F_{2,22}=0.57$ (ns); Hippocampus PHF1: $F_{2,17}=5.98$ (p<0.05); Cortex PHF1: $F_{2,21}=0.41$ (ns); Hippocampus pS409: $F_{2,22}=7.10$ (p<0.01); Cortex pS409: $F_{2,22}=4.62$ (p<0.05). +p<0.05 and +++p<0.001 vs. control condition.

in this region. In conclusion, isoflurane-induced hypothermia quickly triggered tau hyperphosphorylation in the hippocampi and cortices of mice and should be carefully considered during experimental design in tauopathy research to avoid confounding effects on tau phosphorylation.

DISCUSSION

Both pre-clinical and clinical research evaluate tau phosphorylation as a pathological indicator in AD and tauopathies. Our objective was to investigate potential sources of tau phosphorylation
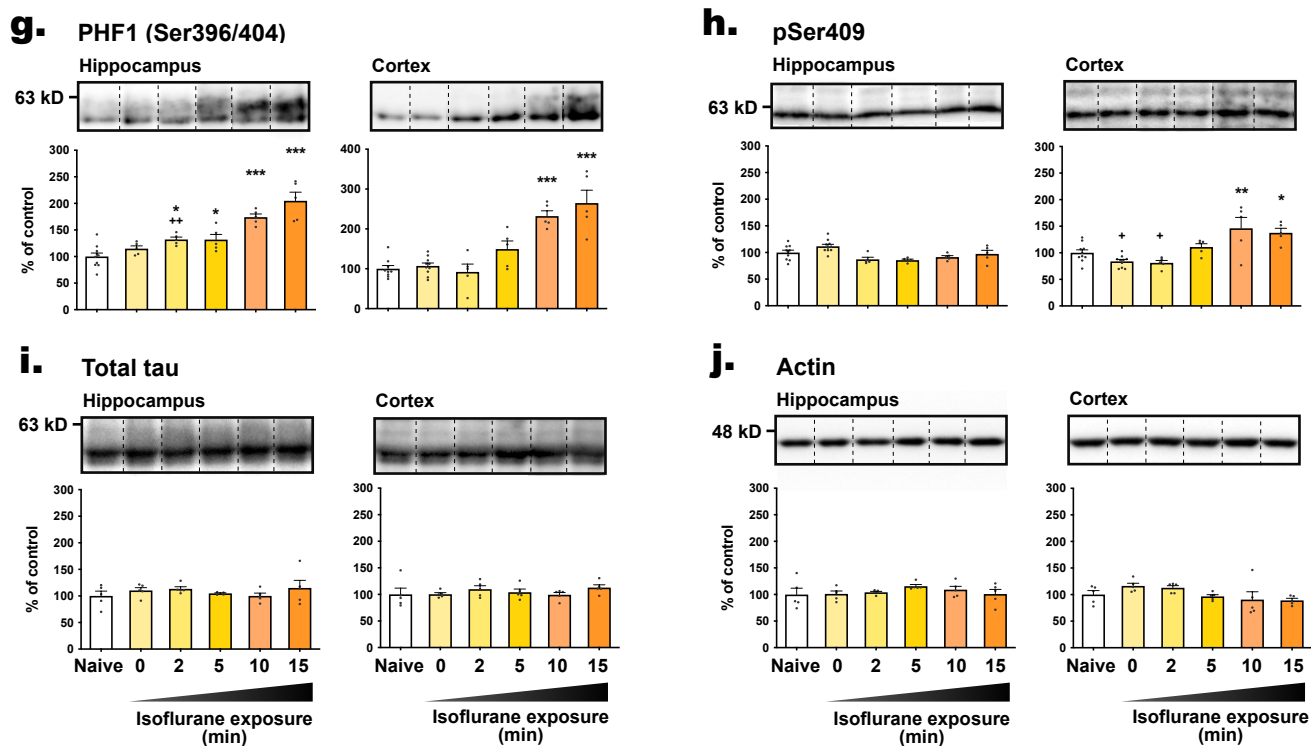
Fig. 6. Continued.

artifacts in animals and cell cultures. To reproduce experimental delays inherent to cell culture protocols, we exposed cells to RT for varying durations prior to sampling. Similarly, we subjected mice to anesthesia-induced hypothermia for comparable periods before euthanasia. In both studies, we observed that hypothermia caused rapid tau hyperphosphorylation at many epitopes. Therefore, to minimize this type of bias in tau-related research, we emphasized the crucial importance of standardizing experimental procedures to eliminate or substantially reduce temperature variations.

Guidance on good cell culture practice highlights the significance of maintaining cells at an optimal and consistent temperature [37]. However, the potential impact of temperature fluctuations during the cell harvesting process has not been explored. When cell plates were removed from the incubator, the cell medium's temperature rapidly decreased within 30 seconds, and this drop continued over time. Within just 5 minutes of removal, significant changes in tau phosphorylation were observed in both SH3R and N2a cells (Table 2). These data corroborate our previous results showing tau hyperphosphorylation in SH3R cells after a 2-hours incubation period at 30°C [38]. In practical terms, this 5-minute timeframe is typically required to process a 6-well plate, highlighting the risk of tau phosphorylation artifacts during simultaneous removal of multiple cell culture dishes from 37°C incubators.

The underlying mechanisms underpinning changes in tau phosphorylation in response to temperature variations have previously been investigated. Our earlier work demonstrated that hypothermia leads to an exponential decrease in tau phosphatase activity juxtaposed with a linear decrease in kinase activity, resulting in tau hyperphosphorylation [4, 14]. However, since our previous studies examined tau phosphorylation over time periods ranging from one to several hours following temperature changes, it is possible that the mechanisms driving hyperphosphorylation may differ within the initial few minutes. To address this concern, we assessed in SH3R cells the expression levels of HSPs, and the activation of GSK3β, JNK, and PP2A, which are all involved in the regulation of tau phosphorylation [32, 33]. Despite stable HSPs expression levels, we observed a rapid activation of GSK3β and JNK, alongside PP2A inhibition, correlating with tau hyperphosphorylation at selective epitopes. With over 20 kinases and 5 phosphatases implicated in tau phosphorylation at various sites [32, 33], delineating the precise regulatory mechanism for each epitope's phosphorylation in response to temperature change remains challenging.

Interestingly, we observed that the N2a cell line manifested a more pronounced and earlier tau hyperphosphorylation relative to SH3R cells (Table 2), potentially reflecting distinct intracellular regulatory or adaptive mechanisms. Notably, a recent study has

Table 2. Time-course alterations of tau phosphorylation in neuronal cell lines exposed at room temperature

Epitope	Cell line	Sampling time (min)					
		0.5	1	2	5	10	15
AT270	SH3R	-3	+7	+34**	+69***	+95***	+76***
	N2a	+52**	+65***	+75***	+90***	+80***	+52*
pSer199	SH3R	+38**	+75***	+75***	+58	+39	+26
	N2a	-10	-0.1	+24*	+30*	+64***	+56***
CP13	SH3R	-12	-27*	-19	-23	+12	+114***
	N2a	+18	+94***	+72***	+75***	+93***	+45*
pThr205	SH3R	-19*	-21**	-8	+1	+20	+43***
	N2a	+17	+36*	+42**	+62**	+118***	+45*
pSer409	SH3R	+16	+11	+10	+15	+45*	+67***
	N2a	+58***	+28*	+29*	+70***	+92***	+51***
AT100	SH3R	+15	+32*	+36*	+50*	+77***	+114***
MC6	SH3R	+23*	+23*	+5	+23	+9	+78***
pSer262	SH3R	+49**	+63***	+55**	+78***	+46*	+82***
PHF1	SH3R	-20**	-22***	-30***	-39***	-35***	+86***
pSer422	SH3R	+20	+32*	+78***	+103***	+136***	+151***

Tau phosphorylation artifacts occurring over minutes was observed in SH3R and N2a cells following their removal from incubation and exposure to room temperature. The values indicate the percentage of phosphorylation changes relative to the baseline control condition (t=0). Significant increases in tau phosphorylation are denoted by a light-yellow background, while significant tau dephosphorylation is represented with a light-blue background. *p<0.05, **p<0.01 and ***p<0.001 vs. control condition.

reported that, while the expression levels of GSK3β were similar between SH-SY5Y and N2a cells, PP2A levels were approximately 50 times higher in SH-SY5Y cells [39]. Additionally, the SH3R cell line features the overexpression of human tau and exhibits a higher basal level of tau phosphorylation [20]. As a result, it might require a higher threshold to achieve detectable hyperphosphorylation. These differences may explain why N2a cells displayed greater sensitivity to tau hyperphosphorylation when exposed to RT. Further investigations are necessary to determine which enzymes are most affected by room temperature exposure in both mouse and human neuronal cells.

Placing cell plates on ice before extraction helped mitigate tau hyperphosphorylation, although this strategy's efficacy diminished as post-incubation time increased. In line with this evidence, we have previously demonstrated that placing mouse brain slices on ice prevents change in tau phosphorylation through enzymatic inhibition [4]. In summary, the rapid temperature changes that occur when removing cell plates from the incubator can lead to unintended tau phosphorylation artifacts. To ensure accurate results, it is crucial to place the cells on ice and to minimize the time between removal from the incubator and performing the required experiments.

Many procedures that induce sedation or anesthesia disrupt thermoregulation [40]. Several anesthetics, including isoflurane, pentobarbital, chloral hydrate, ether, propofol, ketamine/xylazine, halothane, and sevoflurane, have been shown to cause hypothermia and concomitant tau hyperphosphorylation (Table 3). However, the speed at which tau hyperphosphorylation occurs after isoflurane exposure, which is the recommended inhaled anesthetic for animal research according to the American Veterinary Medical Association (AVMA) Guidelines for the Euthanasia of Animals [41], was unknown. In this study, we observed a significant drop in mice's BT during the few seconds required to lose the pedal reflex after isoflurane exposure, resulting in a progressive increase in tau hyperphosphorylation in hippocampi and cortices. After only 10 minutes of isoflurane exposure, the rectal temperature dropped below 30°C, and this was associated with increased phosphorylation of tau at several epitopes. Consequently, exposure to anesthesia can rapidly lower body temperature, leading to artifactual tau hyperphosphorylation.

One potential solution to address this issue is to control the BT of animals with a heating pad [42, 43] or a heated enclosure [44, 45]. However, it is important to note that some anesthetics can induce tau hyperphosphorylation independent of hypothermia. Under normothermic conditions, when BT is monitored and maintained, administration of certain anesthetics like sevoflurane [42], propofol [43, 45] ketamine/xylazine [43], halothane or isoflurane [43, 44] can directly increase tau phosphorylation. Similarly, 30 seconds after inhaling ether or 5 minutes after injecting pentobarbital in mice, tau is hyperphosphorylated at many epitopes, even in the absence of significant changes in BT [16]. The mechanisms underlying normothermic anesthesia-induced tau phosphorylation may involve the effects of anesthetics on kinases and phosphatases [16, 42, 43, 45]. Obviously, the use anesthetic procedure is indispensable in protocols that encompass surgical interventions, as well as in experiments involving intracardiac perfusion for immunohisto-

Table 3. Factors that can influence body temperature and tau phosphorylation

Condition	Protocol	Effect on tau phosphorylation	References
Anesthesia	C57BL/6 mice were anaesthetised with chloral hydrate, pentobarbital sodium or isoflurane	Hyperphosphorylation at AT8 and MC6	14
	JNPL3 mice were exposed acutely or chronically to isoflurane	Hyperphosphorylation at AT8, CP13, MC6, Ser262 and PHF1 and persisted for a week after the last exposure for AT8 CP13, MC6 and Ser262 one week after the last exposure	15
	C57BL/6J mice were anaesthetised with ether inhalation, sodium pentobarbital or propofol	Hyperphosphorylation at Thr181, Ser199, Thr205, Thr212, Ser262, and Ser404	16,65
	Sprague–Dawley rats were anaesthetized with isoflurane for 2h	Hyperphosphorylation at Thr205 and Ser396	17
	hTau mice were Intraperitoneally injected with dexmetomidine	Hyperphosphorylation at AT8, CP13 and PHF1	60
Glucose metabolism	C57BL/6NJcl mice were either starved for 3 days, injected with insulin or with deoxyglucose	Hyperphosphorylation at Ser199, AT8, Thr231, Ser262, Ser396, Ser404 and Ser422	4
	hTau mice were injected with either one high dose (HD) of STZ or 5 low doses (LD) leading to a marked or milder Type1 diabetes mellitus respectively.	Hyperphosphorylation at AT8 and PHF1 for both HD and LD conditions, and Thr205 only for LD group	6
	C57BL/6 mice were injected with STZ	Hyperphosphorylation at pSer199, AT8, AT180, Ser262, Ser356, PHF1, and Ser422 40 days after injection	5
	db/db diabetic mice	Hyperphosphorylation at AT8, CP13 and PHF1	66
	C57BL/6 mice were starved for two days	Hyperphosphorylation at Ser199, AT8, Thr231, Ser262, Ser396, Ser413 and Ser422	3,67
	C57BL/6J male mice were injected with insulin.	Tau phosphorylation was reduced 15 min after the injection and followed by hyperphosphorylation at Ser199, Thr205, Thr212, Ser214, Thr217, Ser262, Ser396 and Ser404	7
Cold water stress	Chinese Kunming mice were forced to swim in ice-cold water for 5 min	Hyperphosphorylation at Ser396	68
	C57BL/6N mice were immersed in ice-cold water for 5 min	Hyperphosphorylation at Ser199, AT8, AT180	69
Physiological temperature changes	Arctic ground or European squirrels were induced into hibernation (moved to a cold chamber and reduction of light duration)	Hyperphosphorylation at AT270, AT8, Thr205, Ser214, AT100, AT180 Ser262, and Ser404	8,9
	Sprague–Dawley rats were induced into synthetic torpor (injection of GABA$_A$ agonist muscimol once an hour for six consecutive times)	Hyperphosphorylation at AT8	10
	During natural sleep phase in C57BL/6N mice	Hyperphosphorylation at AT8, CP13, PHF1, T205, AT180, AT270	11
Heat/cold exposure	C57BL/6J and hTau mice were placed into a ventilated incubator at 42°C for 45 minutes	Dephosphorylation at AT8 and CP13, hyperphosphorylation at Tau1	13
	SH-SY5Y 3R-tau cells were exposed at 40°C for 24 hours	Dephosphorylation at AT8, CP13 and PHF1	
	6- and 18-months C57BL/6N mice were exposed at 4°C for 24 hours	Hyperphoshorylation of tau at CP13, AT180 and AT270 and more importantly in older mice	70
Drugs	Intraperitoneal injection of midalozam (GABA agonist)	Hyperphosphorylation at AT8, CP13, PHF1 and AT180	60
	Intraperitoneal injection of DMSO in mice (4 ml/kg)	Hyperphosphorylation at AT8, PHF, and AT180	63
	Topic administration of 10% menthol in hTau mice	Dephosphorylation at AT8 and PHF1, hyperphosphorylation at Tau1	13

chemistry studies. In such circumstances, we emphasize the imperative need to maintain the BT of the animals, from the induction of anesthesia until the recovery phase, to minimize phosphorylation artifacts. However, it is worth noting that a brief exposure to anesthetics such as isoflurane can also lead to significant changes

in plasma corticosterone, insulin, and glucose levels [46, 47]. This observation is significant because dysfunction in the endocrine stress system and elevated stress hormone levels can contribute to increased tau phosphorylation [48-50]. Similarly, alterations in glucose or insulin metabolism can also promote tau hyperphos-

phorylation [4, 5]. To conclude, whether BT is controlled or not, many anesthetics induce rapid artifactual tau hyperphosphorylation. Therefore, we do not recommend the use of any anesthetic for the euthanasia of laboratory animals when performing experiments examining changes in tau phosphorylation.

Although inhalant anesthetics are considered an acceptable method of euthanasia, CO_2 inhalation is also deemed acceptable according to guidelines from AVMA, Canadian Council of Animal Care (CCAC), and European Union [51]. However, it's important to note that CO_2 inhalation in rodents can lead to a decrease in BT [52, 53] and an increase in kinase activities [54], potentially affecting tau phosphorylation. Moreover, the CCAC recommends using inhalant anesthetics before administering CO_2 [55]. Consequently, similar to anesthesia, CO_2 inhalation has the potential to induce tau phosphorylation artifacts. Our research indicates that, while requiring special authorization and training from an Institutional Animal Care and Use Committee, euthanasia by decapitation or cervical dislocation followed by rapid brain dissection and freezing is the most suitable procedure to avoid tau phosphorylation artifacts. Alternatively, another viable option is euthanasia by Focused Beam Microwave Irradiation, which is in accordance with AVMA Guidelines [51]. This method is particularly effective in preserving physiological protein phosphorylation [56], and the brains are well-suited for Western blotting, ELISA, and immunohistochemistry analysis [57].

Other than anesthesia, various experimental factors can also influence BT and tau phosphorylation (Table 3). Glucose/insulin metabolism alterations [3, 4, 6, 7], the stage of tau pathology progression [58], or the use of certain compounds like midazolam [59, 60], dexmedetomidine [61, 62] or DMSO [63] can lead to tau hyperphosphorylation, with or without hypothermia. Interestingly, hibernation, characterized by significant decreases in BT during prolonged torpor, has been found to induce tau hyperphosphorylation in various animal species [8-10]. Conversely, certain drugs like menthol have the potential to induce thermogenesis, leading to mild hyperthermia and tau dephosphorylation [13]. In conclusion, there are several unexpected factors capable of causing unintentional tau phosphorylation artifacts in laboratory animals. To ensure the accuracy and reliability of tau findings, we strongly advise researchers to record the animal's temperature and incorporate this crucial information in their research publications. By doing so, potential confounding factors related to BT can be considered and controlled for, reducing the risk of reporting erroneous conclusions. This practice will enhance the overall quality and reproducibility of preclinical studies in AD research.

An additional crucial factor to consider in tau studies is the circadian oscillation of BT during the sleep/wake cycle [64]. Recently,

we observed that tau undergoes hyperphosphorylation during the sleep phase when BT is lower, and dephosphorylation occurs during wakefulness when BT increases [11]. This finding necessitates careful consideration in experimental design, as mice are typically euthanized during the light phase when they are asleep. Moving mice within their home cages and initiating experiments can potentially disturb their sleep/wake patterns and BT. Such variations could introduce significant heterogeneity in the subsequent analysis of tau phosphorylation. To address this concern, a simple solution would be to invert the light/dark cycle in animal facilities. By doing so, all animals would be euthanized during their active phase, leading to less fluctuations in BT, and minimizing potential variations in tau phosphorylation (Table 3) [65-70].

CONCLUSION

The analysis of tau phosphorylation, a crucial endpoint in AD research, demands stringent control of experimental variables, particularly temperature fluctuations. This study aimed to raise awareness about the importance of preventing temperature variations in experimental design. Based on our findings, we can confidently recommend the following methods to minimize tau phosphorylation artifacts in cell culture experiments: removing the plates from the incubator individually, placing them on ice, and sampling them immediately. For *in vivo* experiments, we emphasize the significance of recording and documenting BT, and avoiding the use of anesthetic agents before euthanasia. However, in cases where surgical procedures necessitate anesthesia, it is crucial to monitor and maintain BT at 37°C, which helps limit tau hyperphosphorylation. The study recommends decapitation, cervical dislocation, or focused microwave as the preferred methods for euthanasia to ensure the integrity of tau-related researches.

ACKNOWLEDGEMENTS

we are grateful to online Biorender contents for schematic and figures.

DISCLOSURE STATEMENT

DECLARATION OF INTEREST

The authors have no conflict of interest to disclose.

AUTHORS CONTRIBUTIONS

GC and EP designed the study, analyzed the data and wrote the manuscript. GC, ER, FL, EB, IG and PFF performed experiments. All authors reviewed and corrected the manuscript. All authors read and approved the final manuscript.

REFERENCES

1. Long JM, Holtzman DM (2019) Alzheimer disease: an update on pathobiology and treatment strategies. Cell 179:312-339.

2. Selkoe DJ, Hardy J (2016) The amyloid hypothesis of Alzheimer's disease at 25 years. EMBO Mol Med 8:595-608.

3. Yanagisawa M, Planel E, Ishiguro K, Fujita SC (1999) Starvation induces tau hyperphosphorylation in mouse brain: implications for Alzheimer's disease. FEBS Lett 461:329-333.

4. Planel E, Miyasaka T, Launey T, Chui DH, Tanemura K, Sato S, Murayama O, Ishiguro K, Tatebayashi Y, Takashima A (2004) Alterations in glucose metabolism induce hypothermia leading to tau hyperphosphorylation through differential inhibition of kinase and phosphatase activities: implications for Alzheimer's disease. J Neurosci 24:2401-2411.

5. Planel E, Tatebayashi Y, Miyasaka T, Liu L, Wang L, Herman M, Yu WH, Luchsinger JA, Wadzinski B, Duff KE, Takashima A (2007) Insulin dysfunction induces in vivo tau hyperphosphorylation through distinct mechanisms. J Neurosci 27:13635-13648.

6. Gratuze M, Julien J, Petry FR, Morin F, Planel E (2017) Insulin deprivation induces PP2A inhibition and tau hyperphosphorylation in hTau mice, a model of Alzheimer's disease-like tau pathology. Sci Rep 7:46359.

7. Jiang Y, Li L, Dai CL, Zhou R, Gong CX, Iqbal K, Gu JH, Liu F (2020) Effect of peripheral insulin administration on phosphorylation of tau in the brain. J Alzheimers Dis 75:1377-1390.

8. Arendt T, Stieler J, Strijkstra AM, Hut RA, Rüdiger J, Van der Zee EA, Harkany T, Holzer M, Härtig W (2003) Reversible paired helical filament-like phosphorylation of tau is an adaptive process associated with neuronal plasticity in hibernating animals. J Neurosci 23:6972-6981.

9. Su B, Wang X, Drew KL, Perry G, Smith MA, Zhu X (2008) Physiological regulation of tau phosphorylation during hibernation. J Neurochem 105:2098-2108.

10. Luppi M, Hitrec T, Di Cristoforo A, Squarcio F, Stanzani A, Occhinegro A, Chiavetta P, Tupone D, Zamboni G, Amici R, Cerri M (2019) Phosphorylation and dephosphorylation of tau protein during synthetic torpor. Front Neuroanat 13:57.

11. Guisle I, Gratuze M, Petry S, Morin F, Keraudren R, Whittington RA, Hébert SS, Mongrain V, Planel E (2020) Circadian and sleep/wake-dependent variations in tau phosphorylation are driven by temperature. Sleep 43:zsz266.

12. Sultan A, Nesslany F, Violet M, Bégard S, Loyens A, Talahari S, Mansuroglu Z, Marzin D, Sergeant N, Humez S, Colin M, Bonnefoy E, Buée L, Galas MC (2011) Nuclear tau, a key player in neuronal DNA protection. J Biol Chem 286:4566-4575.

13. Guisle I, Canet G, Pétry S, Fereydouni-Forouzandeh P, Morin F, Kérauden R, Whittington RA, Calon F, Hébert SS, Planel E (2022) Sauna-like conditions or menthol treatment reduce tau phosphorylation through mild hyperthermia. Neurobiol Aging 113:118-130.

14. Planel E, Richter KE, Nolan CE, Finley JE, Liu L, Wen Y, Krishnamurthy P, Herman M, Wang L, Schachter JB, Nelson RB, Lau LF, Duff KE (2007) Anesthesia leads to tau hyperphosphorylation through inhibition of phosphatase activity by hypothermia. J Neurosci 27:3090-3097.

15. Planel E, Bretteville A, Liu L, Virag L, Du AL, Yu WH, Dickson DW, Whittington RA, Duff KE (2009) Acceleration and persistence of neurofibrillary pathology in a mouse model of tauopathy following anesthesia. FASEB J 23:2595-2604.

16. Run X, Liang Z, Zhang L, Iqbal K, Grundke-Iqbal I, Gong CX (2009) Anesthesia induces phosphorylation of tau. J Alzheimers Dis 16:619-626.

17. Tan W, Cao X, Wang J, Lv H, Wu B, Ma H (2010) Tau hyperphosphorylation is associated with memory impairment after exposure to 1.5% isoflurane without temperature maintenance in rats. Eur J Anaesthesiol 27:835-841.

18. Chen Z, Wang S, Meng Z, Ye Y, Shan G, Wang X, Zhao X, Jin Y (2023) Tau protein plays a role in the mechanism of cognitive disorders induced by anesthetic drugs. Front Neurosci

17:1145318.

19. Whittington RA, Bretteville A, Dickler MF, Planel E (2013) Anesthesia and tau pathology. Prog Neuropsychopharmacol Biol Psychiatry 47:147-155.

20. Delobel P, Mailliot C, Hamdane M, Sambo AV, Bégard S, Violleau A, Delacourte A, Buée L (2003) Stable-tau overexpression in human neuroblastoma cells: an open door for explaining neuronal death in tauopathies. Ann N Y Acad Sci 1010:623-634.

21. Petry FR, Pelletier J, Bretteville A, Morin F, Calon F, Hébert SS, Whittington RA, Planel E (2014) Specificity of anti-tau antibodies when analyzing mice models of Alzheimer's disease: problems and solutions. PLoS One 9:e94251.

22. Petry FR, Nicholls SB, Hébert SS, Planel E. (2017). A simple method to avoid nonspecific signal when using monoclonal anti-tau antibodies in western blotting of mouse brain proteins. In: Tau protein: methods and protocols (Smet-Nocca C, ed), pp 263-272. Humana Press, New York, NY.

23. Goedert M, Jakes R, Crowther RA, Cohen P, Vanmechelen E, Vandermeeren M, Cras P (1994) Epitope mapping of monoclonal antibodies to the paired helical filaments of Alzheimer's disease: identification of phosphorylation sites in tau protein. Biochem J 301(Pt 3):871-877.

24. Weaver CL, Espinoza M, Kress Y, Davies P (2000) Conformational change as one of the earliest alterations of tau in Alzheimer's disease. Neurobiol Aging 21:719-727.

25. Zheng-Fischhöfer Q, Biernat J, Mandelkow EM, Illenberger S, Godemann R, Mandelkow E (1998) Sequential phosphorylation of tau by glycogen synthase kinase-3β and protein kinase A at Thr212 and Ser214 generates the Alzheimer-specific epitope of antibody AT100 and requires a paired-helical-filament-like conformation. Eur J Biochem 252:542-552.

26. Jicha GA, Bowser R, Kazam IG, Davies P (1997) Alz-50 and MC-1, a new monoclonal antibody raised to paired helical filaments, recognize conformational epitopes on recombinant tau. J Neurosci Res 48:128-132.

27. Otvos L Jr, Feiner L, Lang E, Szendrei GI, Goedert M, Lee VM (1994) Monoclonal antibody PHF-1 recognizes tau protein phosphorylated at serine residues 396 and 404. J Neurosci Res 39:669-673.

28. Augustinack JC, Schneider A, Mandelkow EM, Hyman BT (2002) Specific tau phosphorylation sites correlate with severity of neuronal cytopathology in Alzheimer's disease. Acta Neuropathol 103:26-35.

29. Buée L, Bussière T, Buée-Scherrer V, Delacourte A, Hof PR (2000) Tau protein isoforms, phosphorylation and role in neurodegenerative disorders. Brain Res Brain Res Rev 33:95-

130.

30. Šimić G, Babić Leko M, Wray S, Harrington C, Delalle I, Jovanov-Milošević N, Bažadona D, Buée L, de Silva R, Di Giovanni G, Wischik C, Hof PR (2016) Tau protein hyperphosphorylation and aggregation in Alzheimer's disease and other tauopathies, and possible neuroprotective strategies. Biomolecules 6:6.

31. Thompson AD, Scaglione KM, Prensner J, Gillies AT, Chinnaiyan A, Paulson HL, Jinwal UK, Dickey CA, Gestwicki JE (2012) Analysis of the tau-associated proteome reveals that exchange of Hsp70 for Hsp90 is involved in tau degradation. ACS Chem Biol 7:1677-1686.

32. Martin L, Latypova X, Wilson CM, Magnaudeix A, Perrin ML, Terro F (2013) Tau protein phosphatases in Alzheimer's disease: the leading role of PP2A. Ageing Res Rev 12:39-49.

33. Martin L, Latypova X, Wilson CM, Magnaudeix A, Perrin ML, Yardin C, Terro F (2013) Tau protein kinases: involvement in Alzheimer's disease. Ageing Res Rev 12:289-309.

34. Ichijo H (1999) From receptors to stress-activated MAP kinases. Oncogene 18:6087-6093.

35. Cohen P, Frame S (2001) The renaissance of GSK3. Nat Rev Mol Cell Biol 2:769-776.

36. Querfurth HW, LaFerla FM (2010) Alzheimer's disease. N Engl J Med 362:329-344.

37. Pamies D, Leist M, Coecke S, Bowe G, Allen DG, Gstraunthaler G, Bal-Price A, Pistollato F, de Vries RBM, Hogberg HT, Hartung T, Stacey G (2022) Guidance document on Good Cell and Tissue Culture Practice 2.0 (GCCP 2.0). ALTEX 39:30-37.

38. Bretteville A, Marcouiller F, Julien C, El Khoury NB, Petry FR, Poitras I, Mouginot D, Lévesque G, Hébert SS, Planel E (2012) Hypothermia-induced hyperphosphorylation: a new model to study tau kinase inhibitors. Sci Rep 2:480.

39. Pan B, Lu X, Han X, Huan J, Gao D, Cui S, Ju X, Zhang Y, Xu S, Song J, Wang L, Zhang H, Niu Q (2021) Mechanism by which aluminum regulates the abnormal phosphorylation of the tau protein in different cell lines. ACS Omega 6:31782-31796.

40. Bindu B, Bindra A, Rath G (2017) Temperature management under general anesthesia: compulsion or option. J Anaesthesiol Clin Pharmacol 33:306-316.

41. Leary S, Underwood W, Anthony R, Cartner S, Grandin T, Greenacre C, Gwaltney-Brant S, McCrackin MA, Meyer R, Miller D, Shearer J, Turner T, Yanong R (2020) American Veterinary Medical Association (AVMA) guidelines for the Euthanasia of animals: 2020 edition. AVMA, Schaumburg, IL.

42. Le Freche H, Brouillette J, Fernandez-Gomez FJ, Patin P, Caillierez R, Zommer N, Sergeant N, Buée-Scherrer V, Lebuffe G,

Blum D, Buée L (2012) Tau phosphorylation and sevoflurane anesthesia: an association to postoperative cognitive impairment. Anesthesiology 116:779-787.

43. Hector A, McAnulty C, Piché-Lemieux MÉ, Alves-Pires C, Buée-Scherrer V, Buée L, Brouillette J (2020) Tau hyperphosphorylation induced by the anesthetic agent ketamine/xylazine involved the calmodulin-dependent protein kinase II. FASEB J 34:2968-2977.

44. Tang JX, Mardini F, Caltagarone BM, Garrity ST, Li RQ, Bianchi SL, Gomes O, Laferla FM, Eckenhoff RG, Eckenhoff MF (2011) Anesthesia in presymptomatic Alzheimer's disease: a study using the triple-transgenic mouse model. Alzheimers Dement 7:521-531.e1.

45. Whittington RA, Virág L, Marcouiller F, Papon MA, El Khoury NB, Julien C, Morin F, Emala CW, Planel E (2011) Propofol directly increases tau phosphorylation. PLoS One 6:e16648.

46. Zardooz H, Rostamkhani F, Zaringhalam J, Faraji Shahrivar F (2010) Plasma corticosterone, insulin and glucose changes induced by brief exposure to isoflurane, diethyl ether and CO2 in male rats. Physiol Res 59:973-978.

47. Hsu AA, von Elten K, Chan D, Flynn T, Walker K, Barnhill J, Naun C, Pedersen AM, Ponaman M, Fredericks GJ, Crudo DF, Pinsker JE (2012) Characterization of the cortisol stress response to sedation and anesthesia in children. J Clin Endocrinol Metab 97:E1830-E1835.

48. Green KN, Billings LM, Roozendaal B, McGaugh JL, LaFerla FM (2006) Glucocorticoids increase amyloid-beta and tau pathology in a mouse model of Alzheimer's disease. J Neurosci 26:9047-9056.

49. Canet G, Chevallier N, Perrier V, Desrumaux C, Givalois L (2019). Targeting glucocorticoid receptors: a new avenue for Alzheimer's disease therapy. In: Pathology, prevention and therapeutics of neurodegenerative disease (Singh S, Joshi N, eds), pp 173-183. Springer, Singapore.

50. Canet G, Hernandez C, Zussy C, Chevallier N, Desrumaux C, Givalois L (2019) Is AD a stress-related disorder? Focus on the HPA axis and its promising therapeutic targets. Front Aging Neurosci 11:269.

51. Shomer NH, Allen-Worthington KH, Hickman DL, Jonnalagadda M, Newsome JT, Slate AR, Valentine H, Williams AM, Wilkinson M (2020) Review of rodent euthanasia methods. J Am Assoc Lab Anim Sci 59:242-253.

52. Schaefer KE, Messier AA, Morgan C, Baker GT 3rd (1975) Effect of chronic hypercapnia on body temperature regulation. J Appl Physiol 38:900-906.

53. Granjeiro ÉM, da Silva GS, Giusti H, Oliveira JA, Glass ML, Garcia-Cairasco N (2016) Behavioral, ventilatory and thermoregulatory responses to hypercapnia and hypoxia in the Wistar audiogenic rat (WAR) strain. PLoS One 11:e0154141.

54. Ko MJ, Mulia GE, van Rijn RM (2019) Commonly used anesthesia/euthanasia methods for brain collection differentially impact MAPK activity in male and female C57BL/6 mice. Front Cell Neurosci 13:96.

55. Charbonneau R, Niel L, Olfert E, von Keyserlingk M, Griffin G (2010) Canadian Council on Animal Care (CCAC) guidelines on: euthanasia of animals used in science. CCAC, Ottawa, ON.

56. O'Callaghan JP, Sriram K (2004) Focused microwave irradiation of the brain preserves in vivo protein phosphorylation: comparison with other methods of sacrifice and analysis of multiple phosphoproteins. J Neurosci Methods 135:159-168.

57. Fernandes A, Li YW (2017) Focused microwave irradiation-assisted immunohistochemistry to study effects of ketamine on phospho-ERK expression in the mouse brain. Brain Res 1670:86-95.

58. Maurin H, Lechat B, Borghgraef P, Devijver H, Jaworski T, Van Leuven F (2014) Terminal hypothermic tau.P301L mice have increased tau phosphorylation independently of glycogen synthase kinase 3α/β. Eur J Neurosci 40:2442-2453.

59. Griffiths JW, Goudie AJ (1986) Analysis of the role of drug-predictive environmental stimuli in tolerance to the hypothermic effects of the benzodiazepine midazolam. Psychopharmacology (Berl) 90:513-521.

60. Whittington RA, Virág L, Gratuze M, Lewkowitz-Shpuntoff H, Cheheltanan M, Petry F, Poitras I, Morin F, Planel E (2019) Administration of the benzodiazepine midazolam increases tau phosphorylation in the mouse brain. Neurobiol Aging 75:11-24.

61. Lähdesmäki J, Sallinen J, MacDonald E, Sirviö J, Scheinin M (2003) Alpha2-adrenergic drug effects on brain monoamines, locomotion, and body temperature are largely abolished in mice lacking the alpha2A-adrenoceptor subtype. Neuropharmacology 44:882-892.

62. Whittington RA, Virág L, Gratuze M, Petry FR, Noël A, Poitras I, Truchetti G, Marcouiller F, Papon MA, El Khoury N, Wong K, Bretteville A, Morin F, Planel E (2015) Dexmedetomidine increases tau phosphorylation under normothermic conditions in vivo and in vitro. Neurobiol Aging 36:2414-2428.

63. Julien C, Marcouiller F, Bretteville A, El Khoury NB, Baillargeon J, Hébert SS, Planel E (2012) Dimethyl sulfoxide induces both direct and indirect tau hyperphosphorylation. PLoS One 7:e40020.

64. Harding EC, Franks NP, Wisden W (2020) Sleep and thermo-regulation. Curr Opin Physiol 15:7-13.

65. Xiao H, Run X, Cao X, Su Y, Sun Z, Tian C, Sun S, Liang Z (2013) Temperature control can abolish anesthesia-induced tau hyperphosphorylation and partly reverse anesthesia-induced cognitive impairment in old mice. Psychiatry Clin Neurosci 67:493-500.

66. El Khoury NB, Gratuze M, Petry F, Papon MA, Julien C, Marcouiller F, Morin F, Nicholls SB, Calon F, Hébert SS, Marette A, Planel E (2016) Hypothermia mediates age-dependent increase of tau phosphorylation in db/db mice. Neurobiol Dis 88:55-65.

67. Planel E, Yasutake K, Fujita SC, Ishiguro K (2001) Inhibition of protein phosphatase 2A overrides tau protein kinase I/ glycogen synthase kinase 3 beta and cyclin-dependent kinase 5 inhibition and results in tau hyperphosphorylation in the hippocampus of starved mouse. J Biol Chem 276:34298-34306.

68. Feng Q, Cheng B, Yang R, Sun FY, Zhu CQ (2005) Dynamic changes of phosphorylated tau in mouse hippocampus after cold water stress. Neurosci Lett 388:13-16.

69. Okawa Y, Ishiguro K, Fujita SC (2003) Stress-induced hyperphosphorylation of tau in the mouse brain. FEBS Lett 535:183-189.

70. Tournissac M, Vandal M, François A, Planel E, Calon F (2017) Old age potentiates cold-induced tau phosphorylation: linking thermoregulatory deficit with Alzheimer's disease. Neurobiol Aging 50:25-29.